

HIGH-PERFORMANCE EXOPLANET TRANSIT FITTING

SYDNEY JENKINS

Github link: https://github.com/sydneyjenkins/Julia_Project

Abstract. Discovering exoplanets with the transit technique requires continuous monitoring of $O(100,000)$ stars. It is therefore critical to have an efficient, automated pipeline for identifying the dips in brightness characteristic of stars with transiting exoplanets. We perform a preliminary investigation of whether a Julia fitting pipeline could fulfill this role by comparing the speed of Python and Julia implementations and comparing the accuracy of two different fitting models, called the Box model and the Mandel-Agol model. These models are fit using our own Markov chain Monte Carlo sampler. We find that the Julia implementation outperforms the Python implementation, and that parallelization provides an additional increase in speed. Additionally, more complex models require a trade-off between accuracy and efficiency.

1. Introduction. Since the first discovery of the first exoplanet in 1992 [5], over 5,000 exoplanets have been discovered. Nearly 4,000 of these worlds were found using transit techniques [e.g., 1]. As a planet orbits around its host star, it blocks a portion of its light. This signal is detectable in the system’s brightness as a function of time, commonly known as the light curve. The change in brightness is closely related to the relative sizes of the planet r_p and star r_* , and is proportional to $(\frac{r_p}{r_*})^2$. Figure 1 provides a demonstration of how the exoplanet’s motion affects the observed light curve. This light curve encodes important information about the system, such as the planet’s orbital period, radius, and density (when combined with stellar radial velocity data).

In order to find exoplanets using the transit method, many stars must be monitored. For instance, past missions such as Kepler observed $O(100,000)$ stars, while future missions such as the Nancy Grace Roman Space Telescope plan to observe $O(100,000,000)$ stars. Being able to efficiently fit a large number of light curves will therefore be critical for quickly identifying exoplanets hidden in upcoming telescope data.

We conduct a preliminary investigation into whether Julia would provide a suitable platform for creating a transit fitting pipeline. To do this, we create a Julia pipeline to test the accuracy and efficiency of different fitting methods. Specifically, we test two different transit models: the Box model and the Mandel-Agol model. We also run our code using Python and Julia implementations, and serial and parallel implementations. We then compare the speed and accuracy of our different implementations. To fit our models, we write our own Markov chain Monte Carlo sampler.

The paper is organized as follows. We describe our data in section 2, our fitting models in section 3, and our MCMC sampler in section 4. Our experimental set-up is outlined in section 5, results are discussed in section 6, code availability is described in section 7, and future work is proposed in section 8. We then conclude in section 9.

2. Data. We use data from Kepler, a space-based telescope that operated between 2009 and 2018. Kepler had a fixed field of view, meaning that it continuously looked at the same patch of sky. It monitored $\sim 150,000$ stars in this region. This long-term monitoring of a large number of stars makes it the ideal mission for studying transiting exoplanets.

We place several restrictions on the light curves used in this analysis. We focus on bright targets (with magnitudes < 14) and easily-observed transit depths (0.01 – 0.05) that correspond to large planets. This period depth is defined as the fractional

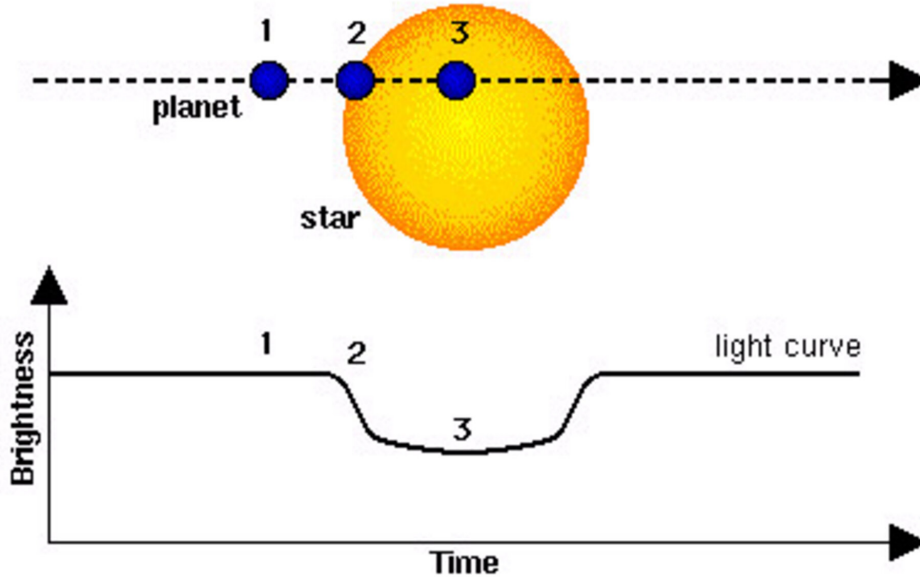


FIG. 1. Diagram depicting an exoplanet transit. If the star, planet, and observer are properly aligned, we observe a dip in the star’s brightness as the planet passes in front of it. Position 1, 2, and 3 correspond to the out-of-transit brightness, ingress brightness, and in-transit brightness, respectively. Diagram from the European Space Agency (ESA).

49 change in flux during the transit. We also require that the planet’s orbital period is
 50 greater than 5 days, as this avoids light curves with unusual shapes. In future work,
 51 these constraints could be loosened in order to fit a wider variety of light curves. This
 52 is further discussed in [section 8](#). 115 Kepler stars with known planets satisfy our
 53 magnitude, depth, and period constraints. Several example light curves are shown
 54 in Figure 2. These light curves all correspond to different planet sizes, periods, and
 55 orbital configurations.

56 Each light curve in our sample is normalized using a package called `keplersplinev2`
 57 [4]. This package also smooths the light curve and removes long-term variability
 58 caused by stellar effects and instrumental artifacts.

59 In this analysis, we choose to divide each light curve into individual transit events,
 60 rather than fitting the entire light curve or fitting the phase-folded light curve. This
 61 was done to minimize the fitting time. While this reduction in our data size may
 62 reduce the quality of our fit, it still provides a sufficient basis for this preliminary
 63 investigation, as we can still compare the calculated running times and accuracy
 64 measurements of the different fitting methods.

65 **3. Fitting Algorithms.** To investigate the trade-off between speed and accu-
 66 racy, we compare two exoplanet transit models: the Box model and the Mandel-Agol
 67 model. This allows us to explore the effects of model complexity on both the running
 68 time and accuracy of our fitting code. These models are described in detail below.

69 **3.1. Box Model.** The Box model is the simplest exoplanet transit fitting model.
 70 It models the transit event as a box-shaped function that takes either a high (out-of-
 71 transit) or low (in-transit) value. It requires four parameters: the period P , transit

72 duration ΔT , transit depth d , and a reference time t_0 . Because we are only fitting
 73 an individual transit, our input data does not contain information about the planet's
 74 orbital period. We therefore use the Kepler catalogue period for this initial investiga-
 75 tion. Additionally, while the reference time normally corresponds to some mid-transit
 76 time of an earlier transit, in this case we define it as the starting time of the observed
 77 transit. Our Box function is therefore a piece-wise function of the following form:

$$78 \quad (3.1) \quad F(t, t_0, \Delta t, d) = \begin{cases} 1 & \text{if } t < t_0 \text{ or } t > t_0 + \Delta t \\ 1 - d & \text{if } t > t_0 \text{ and } t < t_0 + \Delta t \end{cases}$$

79 F corresponds to the observed stellar flux. This equation assumes that the light curve
 80 has been normalized to a value of 1.

81 **3.2. Mandel-Agol Model.** The Mandel-Agol (MA) model [3] is a more com-
 82 plex model for fitting exoplanet transits. Specifically, this model accounts for an
 83 optical effect called limb darkening. This occurs because, when looking at a star
 84 closer to its center, one can see further into its atmosphere. Because these deeper
 85 layers are at a higher temperature, the star appears brighter. Therefore, stars will
 86 seem brighter at their center and dimmer at their edges, or “limbs.” This effect is
 87 visible in Figure 1. Because of limb darkening, when the planet passes in front of the
 88 edges of the star, it will block less flux than it does when it passes in front of the
 89 center of the star. This causes the light curve to become more rounded.

90 We model this effect using a quadratic limb darkening model. This impacts the
 91 stellar intensity I , which is defined in terms of the limb darkening coefficients (γ_1 and
 92 γ_2) and μ (where $\mu = \sqrt{1 - r^2}$). μ accounts for the changing angle between the planet
 93 and star. Specifically, I is defined as:

$$94 \quad (3.2) \quad I(\gamma_1, \gamma_2, \mu) = 1 - \gamma_1(1 - \mu) - \gamma_2(1 - \mu)^2$$

95 To establish a baseline, we also model the flux ratio for a uniform source $F^e(p, z) =$
 96 $1 - \lambda^e(p, z)$. This value depends on the size ratio between the planet and star p and
 97 the normalized separation of the object centers z . Specifically, p is defined in terms
 98 of the planetary radius r_p and stellar radius r_* to be r_p/r_* . z is defined in terms of
 99 the center-to-center distance between the star and planet d and the stellar radius to
 100 be d/r_* . λ^e is defined below:

$$101 \quad (3.3) \quad \lambda^e(p, z) = \begin{cases} 0 & \text{if } 1 + p < z \\ \frac{1}{\pi} \left[p^2 \kappa_0 + \kappa_1 - \sqrt{\frac{4z^2 - (1+z^2 - p^2)^2}{4}} \right] & \text{if } |1 - p| < z \leq 1 + p \\ p^2 & \text{if } z \leq 1 - p \\ 1 & \text{if } z \leq p - 1 \end{cases}$$

102 The parameters κ_0 and κ_1 are defined as $\cos^{-1}[(p^2 + z^2 - 1)/2pz]$ and $\cos^{-1}[(1 - p^2 +$
 103 $z^2)/2pz]$, respectively.

104 We then combine these equations to define the final light curve:

$$105 \quad (3.4) \quad F(r, p, z) = \left[\int_0^1 2rI(r) dr \right]^{-1} \int_0^1 I(r) \frac{d[F^e(p/r, z/r)r^2]}{dr} dr$$

106 F and r correspond to the observed stellar flux and the normalized radial coordinate
 107 on the disk of the star, respectively. We note that this gives the flux as a function of

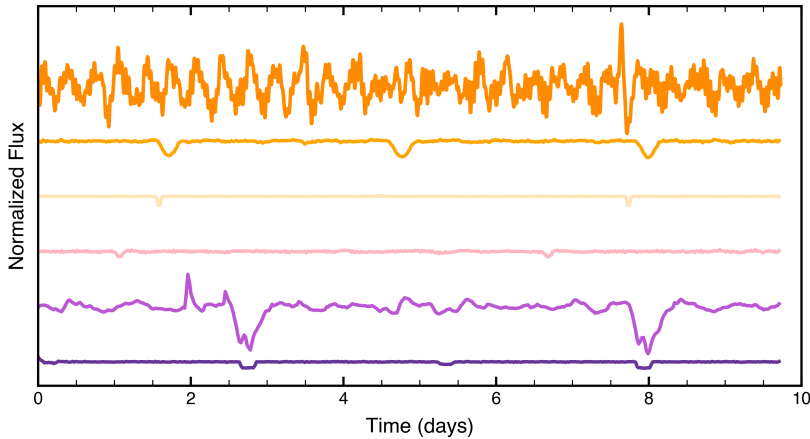


FIG. 2. Example exoplanet transits from Kepler data, shown as the normalized stellar flux as a function of time. The passage of the planet in front of the star is detectable as a periodic dip in the host star’s flux. Different planet sizes and orbital configurations create a diverse variety of light curve shapes.

108 position instead of time. To convert this to a function of time, we use the following
 109 equation for z :

$$110 \quad (3.5) \quad z(t) = R_a^{-1} [(\sin\omega t)^2 + (\cos i \cos\omega t)^2]^{1/2}$$

111 Here, R_a is the stellar radius over the planet’s semi-major axis, i is the inclination
 112 angle, and ω is $\frac{2\pi}{P}$, where P is the planet’s orbital period.

113 Because we are only fitting a single transit, rather than a full light curve or phase-
 114 folded transit, we expect there to be degeneracies between these many parameters. We
 115 therefore simplify the fitting process by assuming that the star, planet, and observer
 116 are perfectly aligned ($i = 0$). We also use the value of the period provided by the
 117 Kepler catalog. We therefore restrict ourselves to fitting the following parameters:
 118 the time of transit t_0 , γ_1 , γ_2 , p , and R_a .

119 **4. MCMC Fitting.** We write our own Markov chain Monte Carlo (MCMC)
 120 sampler to find the best-fit parameters. We create multiple walkers to explore the
 121 parameter space, all starting from slightly different starting guesses. Each walker has
 122 their own corresponding chain, where they can update their parameter values.

123 We update each set of parameters by adding a small perturbation. We then
 124 calculate the acceptance probability of this new state using the log likelihood function
 125 and log prior function. The log likelihood function computes the logarithm of the
 126 likelihood of observing the data given the current set of model parameters. Taking
 127 the logarithm simply simplifies the calculations performed. However, maximizing the
 128 log likelihood function is equivalent to maximizing the likelihood function. We can
 129 therefore use it to determine whether one set of parameters is a better fit than another
 130 set of values.

131 The priors restrict the parameters to certain allowed ranges. For both the Box
 132 and MA model, we allow t_0 to range within 0.2 days of a pre-calculated value. This is
 133 meant to simplify the fitting process. For the Box model, we then allow Δt to range

134 between 0.01 and 0.5 days, and d to range between 0.01 and 0.1. For the MA model,
 135 we allow γ_1 and γ_2 to range between -1 and 1, p to range between 0 and 0.5, and R_a
 136 to range between 0.001 and 1.

137 Once we have calculated the sum of the log likelihood and log prior values for a
 138 given iteration i , denoted by l_i , we can determine the acceptance probability. This
 139 is calculated by taking the difference with the previous sum (i.e. $l_i - l_{i-1}$). We then
 140 generate a random number n to determine whether the new parameter values are
 141 accepted ($l_i - l_{i-1} > \log(n)$) or rejected ($l_i - l_{i-1} < \log(n)$). In this way, the sampler
 142 will converge toward increasingly better fitting parameter values.

143 After a set number of iterations, some number of parameter values are discarded
 144 from each chain in a process known as burn-in. This allows us to take the mean and
 145 standard deviation of the chains after they have reached some equilibrium value, thus
 146 providing us with the best-fit parameter values.

147 Two example fits are shown in Figure 3. This figure showcases both the Box and
 148 MA models, both fit to the transit data of star KIC 6965293 (shown in black) using
 149 our MCMC code. The best-fit parameter values are also provided.

150 5. Experimental Set-Up.

151 **5.1. Comparisons.** We perform several comparisons in this investigation. These
 152 are summarized below:

- 153 • **Python vs. Julia** We implement our algorithms in both Python and Julia. This
 154 is done to compare the speed of calculations in each language. We expect
 155 the Julia implementations to be faster, given that Julia was designed for
 156 efficiency.
- 157 • **Box vs. MA Model** We fit our light curves with both the Box and MA model.
 158 The Box model requires us to fit only three parameters, while the MA model
 159 requires us to fit five parameters. The MA model is also significantly more
 160 computationally expensive, as it requires many more computations, including
 161 two integrals. We therefore expect it to take a longer time to perform each
 162 iteration. However, we also expect it to provide a better fit to the data, as it
 163 accounts for limb darkening effects.
- 164 • **Serial vs. Parallel** We fit each model using both a serial and parallel implemen-
 165 tation, allowing us to investigate the benefits of parallelization. Because we
 166 are running this pipeline locally, we only use four threads (corresponding to
 167 the number of cores on our machine). However, we still expect to observe a
 168 speedup for the parallel implementation.

169 **5.2. Measurements.** In this experiment, we are interested in the speed and
 170 accuracy of our implementations. We estimate these parameters using the methods
 171 described below:

- 172 • **Speed** To perform a fair comparison of algorithm speeds, we time each implemen-
 173 tation using the same number of walkers and iterations per walker. Because
 174 Python is slow, we limit ourselves to 128 walkers and 100 iterations per walker
 175 for the comparison between Python and Julia. We then time the MCMC
 176 code, using the time modules in Python and Julia. We decide not to use the
 177 Julia BenchmarkTools package in order to provide a fairer comparison with
 178 the Python time measurements. We acknowledge that, given the relatively
 179 small (12800) number of total parameter updates performed per implementa-
 180 tion in this experiment, the estimated times include large contributions from
 181 the MCMC overhead calculations, such as determining the initial parameter

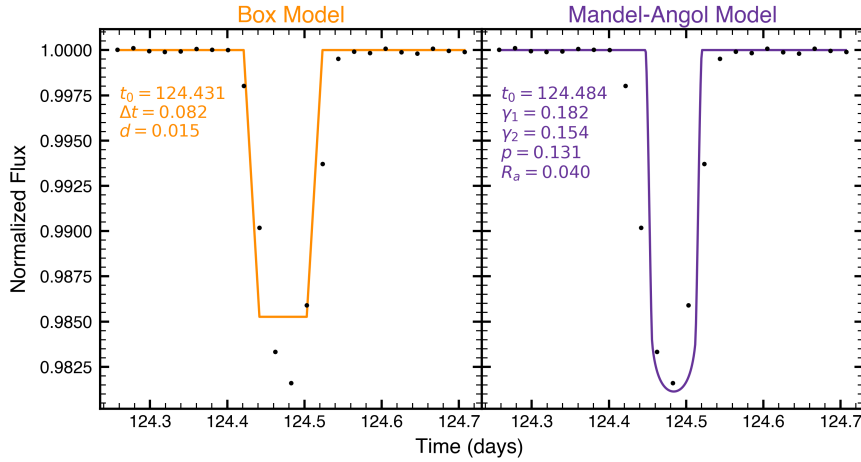


FIG. 3. Example model fits to star KIC 6965293. Data is shown in black. The best-fit parameter values and fit are shown for the Box model (left) and for the Mandel-Agol (MA) model (right). The MA model provides a more accurate fit to the transit event, but is more computationally expensive.

- 182 guesses and initializing the chains. To provide a better comparison of the
 183 time requirements for the Julia implementations, we also measure the time
 184 taken to compute 10,000 iterations per walker.
- 185 • **Accuracy** To estimate the accuracy of a given fit, we calculate the Root Mean
 186 Square Error (RMSE) of the model’s predictions. The RMSE is calculated
 187 using the following equation:

$$188 \quad (5.1) \quad RMSE = \sqrt{\frac{\sum_{i=1}^n (\hat{y}_i - y_i)^2}{n}}$$

189 where n is the size of the data set, y_i is the i th data point, and \hat{y}_i is the i th
 190 model prediction. Because the average RMSE is expected to be the same for
 191 a given model, regardless of whether the model is fit in Julia or Python, or fit
 192 using a serial or parallel implementation, we simply calculate a mean RMSE
 193 using our parallel Julia implementation. We fit 20 unique transits and use
 194 the mean RMSE values to compare the accuracy of the Box and MA models.

195 **6. Results and Discussion.** We measure the time per iteration for each of
 196 eight implementations, and the RMSE for both the Box and Mandel-Agol models.
 197 Our results are summarized in [Table 1](#).

198 We find that the Julia implementation is faster, as expected. Specifically, we find
 199 that the speed of the Julia implementations is ~ 3 orders of magnitude faster than the
 200 corresponding Python versions. This indicates that Julia would be a suitable language
 201 for large-scale exoplanet transit fitting, as it would be able to efficiently fit the large
 202 number of light curves that will be generated by upcoming telescope missions.

203 We also find that parallelizing the Julia code provides an additional speed-up
 204 for the 10,000-iteration comparison. This is consistent with what we expected, as
 205 having multiple threads iterate over the chains reduces the overall time required to
 206 perform all the computations. We find that the serial versions take 1.4 and 2.7

207 times longer than the parallel versions when fitting the Box model and MA models,
 208 respectively. However, the increased speed is less than one might naively expect when
 209 using four threads. That is, even though we use four threads, our code does not run
 210 four times faster. This makes sense, as there are computational overheads to both our
 211 fitting algorithm (such as initializing the chains) and the process of multi-threading
 212 (such as creating multiple threads). This also explains why, in the 100-iteration
 213 comparison, the parallel version sometimes performs worse than the serial version—
 214 with a lower number of iterations per walker, the advantage gained by parallelizing
 215 the code becomes dominated by the overhead costs.

216 Finally, we find that fitting the Box model is ~ 2 orders of magnitude faster
 217 than fitting the MA model. This is also consistent with our expectations, as the
 218 Box model has fewer parameters to fit and requires fewer computations. However,
 219 there is a trade-off between speed and accuracy, as the MA model has a lower RMSE
 220 (0.002 ± 0.001) compared to the Box model (0.003 ± 0.002). This performance reflects
 221 the MA model’s inclusion of limb darkening effects. These results indicate that, when
 222 choosing which model to fit to a light curve, it is important to consider the relative
 223 importance of speed compared to accuracy.

TABLE 1

Results for each method used, including for different languages (Julia or Python), models (Box model or Mandel-Agol model), and computing methods (serial or parallel). We report the time taken to fit a single transit based on the number of iterations per chain (either 100 or 10,000), and the root-mean-square error (RMSE).

Model	Language	P/S	100-it Time (s)	10,000-it Time (s)	RMSE
Box	Julia	Serial	0.03	2.1	0.003 ± 0.002
		Parallel	0.09	1.5	
	Python	Serial	52.1		
		Parallel	49.9		
Mandel-Agol	Julia	Serial	3.9	365.7	0.002 ± 0.001
		Parallel	1.3	131.7	
	Python	Serial	2638.5		
		Parallel	2926.7		

224

225 **7. Code Availability.** The relevant code is included in the GitHub link pro-
 226 vided at the beginning of this study. The GitHub page includes six files, including the
 227 Julia implementation, the Python implementation, and the data. The Julia imple-
 228 mentation includes fits to both the Box and MA models, and includes both serial and
 229 parallel options. The Python implementation includes many of the same functions,
 230 but in Python. Both implementations are done in an interactive format (Pluto and
 231 Jupyter Notebook for the Julia and Python implementations, respectively).

232 Finally, the data files include 115 transits from the stars that satisfy all the criteria
 233 described in [section 2](#). There are also additional files containing the t_0 values, transit
 234 depths, and orbital periods for each light curve. The transit depths and orbital periods
 235 are collected from the Kepler catalog, while the t_0 values are estimated during the
 236 separation of the 115 light curves into individual transit events. These values are used
 237 to help improve our fits, but would ideally not be necessary in the final implementation
 238 of any fitting pipeline.

239 **8. Future Work.** Because this is a preliminary investigation into the benefits
 240 of using a Julia pipeline, there are many areas for future work to expand upon these
 241 results. Specifically, we limit ourselves to a subset of the available light curves, and
 242 only investigate two transit models. Additionally, we use a relatively simple MCMC
 243 sampler, and restrict ourselves to just four threads. We describe ways to address these
 244 limitations in further detail below.

245 • **Increased Diversity of Light Curves** In this experiment, we select light curves
 246 that satisfy the following constraints: $P > 5$ days, magnitude < 14 , and tran-
 247 sit depth between 0.01 and 0.05. This restricted our light curves to those with
 248 relatively straight-forward, easily detectable signals. We additionally only fit
 249 individual transit events. However, to identify transits in real survey data,
 250 we would want to expand our pipeline to be able to fit full light curves with
 251 more complex shapes. Therefore, future work could evaluate the accuracy of
 252 the Box and MA models on a representative set of light curves. Addition-
 253 ally, rather than fitting a single transit, they could fit the entire light curve.
 254 This would allow future implementations to fit the planet’s orbital period, in
 255 addition to the other parameters.

256 • **Additional Transit Models** We could also compare the speed and accuracy of
 257 other exoplanet transit models. Additional parameters that could be fit in-
 258 clude the inclination (which is included in the MA model, but set to a value
 259 of zero in this study), eccentricity, and period. Additionally, there are a wide
 260 range of limb darkening model that can be adopted, including uniform, linear,
 261 logarithmic, and exponential models. Fitting more parameters would allow
 262 us to account for a larger range of behavior in the light curves, thus provid-
 263 ing us with better fits and making our code applicable to a more diverse set
 264 of light curves. Packages that allow for these complexities already exist in
 265 Python [2] and are widely used. A similar implementation in Julia would
 266 provide similar accuracy paired with improved efficiency.

267 • **Optimized Sampler** In addition, we could further optimize our sampler. For
 268 instance, we are currently using a set perturbation distribution to update
 269 our parameter values. However, future work could have an update value
 270 that decreases in size as the sampler converges on the best-fit values. This
 271 would provide a more precise estimate of the best-fit parameters. Similarly,
 272 we could break the fitting into multiple stages, using the average chain values
 273 from the previous iteration as the starting parameters for the next iteration.
 274 The perturbations could then be modified for each of these iterations. This
 275 could also provide improved convergence.

276 • **Increased Parallelization** In this experiment, we restrict the number of threads
 277 to the number of cores on our local machine. However, future work could
 278 run our code on a computing cluster and dramatically increase the amount of
 279 parallelization. This would likely greatly increase the speed of our code. We
 280 would expect that, as we increase the number of threads, the benefit of using
 281 parallelization would increasingly dominate the associated overhead cost of
 282 setting up the parallelization. However, once the number of threads is equal
 283 to the number of walkers, there would no longer be any more advantages to
 284 increasing the number of threads, as the code is designed to designate at least
 285 one walker per thread.

286 **9. Conclusions.** We perform a preliminary comparison of the speed and effi-
 287 ciency of several exoplanet transit fitting methods, with a specific focus on the effects

288 of the coding language, the transit model used, and parallelization. As expected, we
289 find that using Julia and multithreading both lead to increases in speed. Additionally,
290 we find that the MA model provides a more accurate fit to light curve data. However,
291 it also takes longer to fit, indicating that its computational costs should be weighed
292 against its improved accuracy when deciding which model to use. All relevant code
293 is provided on GitHub.

294 Our findings indicate that a Julia transit fitting pipeline could provide improved
295 accuracy relative to more traditional pipelines in Python. As future telescope mis-
296 sions look at an ever increasing number of stars, this efficiency will become a pivotal
297 advantage, making Julia the ideal language for future transit fitting.

298 **References.**

- 299 [1] D. Charbonneau, T. M. Brown, D. W. Latham, and M. Mayor. Detection of
300 Planetary Transits Across a Sun-like Star. , 529(1):L45–L48, Jan. 2000.
- 301 [2] L. Kreidberg. ttbatman/tt: BAsic transit model cAlculationN in python. *Publica-*
302 *tions of the Astronomical Society of the Pacific*, 127(957):1161–1165, nov 2015.
- 303 [3] K. Mandel and E. Agol. Analytic Light Curves for Planetary Transit Searches. ,
304 580(2):L171–L175, Dec. 2002.
- 305 [4] A. Vanderburg and J. A. Johnson. A Technique for Extracting Highly Precise
306 Photometry for the Two-Wheeled Kepler Mission. , 126(944):948, Oct. 2014.
- 307 [5] A. Wolszczan and D. A. Frail. A planetary system around the millisecond pulsar
308 PSR1257 + 12. , 355(6356):145–147, Jan. 1992.